N_{Pr} = Prandtl number
N_{Re} = Reynolds number

LITERATURE CITED

1. Colburn, A. P., and W. J. King, *Ind. Eng. Chem.*, **23**, No. 8, 919 (1931).
2. Koch, Rudolf, *Ver. Deut. Ing.-Forschungsh.*, **24B**, 469, 1 (1958).
3. Kreith, Frank, and David Margolis, *Appl. Sci. Res.*, **8A**, 457 (March, 1959).
4. Gambill, W. R., and R. D. Bundy, *ASME 62-HT-42*, (1962).
5. Seymour, E. V., B.E. thesis, Univ. Western Australia, Applecross (1962).
6. Smithberg, E., and F. Landis, *J. Heat Transfer*, **86**, No. 1, 39 (Feb., 1964).
7. Lopina, R. F., and A. E. Bergles, Mass. Inst. Tech., Tech. Rept. 70281-47 (June, 1967).
8. Thorsen, R., and F. Landis, *ASME 67-HT-24*, (1967).
9. Gambill, W. R., et al., *U. S. At. Energy Comm. Rept. ORNL-2911*, Oak Ridge Natl. Lab., Tenn. (March 28, 1960).
10. Poppendiek, H. F., W. R. Gambill, and N. D. Greene, *Proc. Intern. Conf. Peaceful Uses At. Energy, 3rd Geneva* (1964).
11. Humble, L. V., W. H. Lowdermilk, and L. G. Desmon, *Nat. Advisory Comm. Aeron. Rept. 1020* (1951).
12. Taylor, M. F., and T. A. Kirchgessner, *Nat. Aeron. Space Admin. TN D-133* (Oct., 1959).
13. Ward Smith, A. J., *J. Royal Aeron. Soc.*, **66**, 397 (June, 1962).
14. Dalle-Donne, M., and F. W. Bowditch, *Dragon Project Rept. DP-184*, At. Energy Estab., Winfrith, Eng. (April, 1963).
15. Lel'chuk, V. L., and G. I. Elfimov, *High Temp.*, **2**, No. 2, 214 (1964).
16. Taylor, M. F., *Nat. Aeron. Space Admin. TN D-2280*, (April, 1964).
17. ———, *ibid., TN D-2595*, (Jan., 1965).
18. Petukhov, B. S., et al., *High Temp.*, **3**, No. 1, 91 (1965).
19. Petukhov, B. S., et al., *Proc. 3rd Intern. Heat Transfer Conf., Chicago*, Vol. I, 285, AIChE, New York (1966).
20. Ter-Oganes'yants, A. A., and S. N. Shorin, *Thermal Eng.*, **12**, No. 2, 112 (Feb., 1965).
21. Perkins, H. C., and P. Worsoe-Schmidt, *Int. J. Heat Mass Transfer*, **8**, 1011 (1965).
22. Hilsenrath, Joseph, et al., "Tables of Thermal Properties of Gases," Nat. Bur. Standards Circular 564, (November 1, 1955).

Manuscript received November 17, 1967; revision received March 15, 1968; paper accepted April 26, 1968. Paper presented at AIChE Tampa meeting.

A Study of the Effects of Internal Rib and Channel Geometry in Rectangular Channels

Part I. Pressure Drop

RALPH A. BUONOPANE and RALPH A. TROUPE

Northeastern University, Boston, Massachusetts

Plexiglas models of rectangular channels were fabricated with various rib shapes to determine the effects of rib and channel geometry on the pressure drop. Pressure drops in twenty-four individual variations of channel geometry were investigated using plexiglas models.

From this investigation, an empirical correlation for the pressure drop across the ribbed section of the channel was determined as a function of the linear fluid velocity and the geometric characteristics of the channels. This empirical correlation involves functions of seven geometric parameters of rib pattern and channel geometry.

Ribbed section pressure drops for commercial plate heat exchanger channels were predicted using the geometric characteristics of the commercial plates with the empirical correlations developed from the plexiglas channel studies. The total pressure drop for commercial channels was predicted by adding an average entrance and exit pressure drop to the predicted ribbed section pressure drop.

The correlations developed in this work allow one to determine the pressure drop in a ribbed rectangular channel from the geometric characteristics of the ribs and the channel in question.

Rectangular channels with internal geometries for turbulence promotion have been used for many years in the form of plate and frame heat transfer equipment. Little information has been presented in the literature regarding pressure drop in such channels. The effects of these internal geometries which give ribbed channels quite unique heat transfer characteristics were experimentally investigated. This paper presents the results of these studies in the form of empirical correlations of pressure drop as functions of the rib and channel geometry.

The literature on plate heat exchangers is quite extensive but mainly confined to reporting the technical aspects of particular commercial units. General descriptions of the history and use of plate heat exchangers are presented by Troupe, et al. (*1*) and Seligman and Dummett (*2*). For pressure drop in plate heat exchangers, Baranovskii (*3*) presents a comprehensive work based on the results of many investigations. He presents correlations in the form of $N_{Eu} = A \cdot N_{Re}{}^{-N}$ for many types of plate heat exchanger channels. This type of correlation, however, is useful only for the particular plate channel for which it was obtained. Watson, et al. (*4*) present similar correlations obtained from experimental work with channels composed of a flat plastic plate and a ribbed metal plate.

Recent investigations with plastic prototypes of plate heat exchanger channels indicate that the geometry of the ribs governs the pressure drop in the flow channels. Smith and Troupe (5) present data showing the variation in plate separation for a single rib geometry. Maslov (6) investigated the effects of rib base angle and plate separation on the pressure drop in ribbed plastic channels. His results are presented by the equation:

$$f_B = A \cdot N_{Re}^{-N} \tag{1}$$

where

$$A = 28.8\left(\frac{B}{Y} - 2\right)^{1/3} \tan^{1.33}\beta' \tag{2}$$

$$N = 0.38\left(\frac{B}{Y} - 2\right)^{0.189} \tag{3}$$

This correlation, which indicates the effect of rib geometry on the Blasius frictional parameter, f_B, is useful only for triangular shaped close-packed ribbed channels. In another work with plastic plates, Maslov (7) investigated the effects of rib spacing or frequency and plate separation in triangular ribbed channels but applied his results to evaluate the critical Reynolds number in such channels. He found that the rib frequency, another aspect of channel geometry, also affected the pressure drop in a plate heat exchanger channel. His results, presented by the correlation:

$$(N_{Re})_{\text{crit.}} = 2{,}900\left(\frac{F^2_{\min}}{F \cdot Y}\right)^{-2/3} \tag{4}$$

show that the critical Reynolds number in ribbed channels is always less than 2,900 and in most situations, less than 1,000.

A purely theoretical analysis of flow in channels of the type in question is virtually impossible because of the extremely complex flow patterns (5). Pressure losses across the ribbed section of these channels may be caused by the numerous expansion and contraction losses, numerous eddy formations behind the ribs, numerous turns of the main flow stream due to channel curvatures, and skin friction losses common to metal surfaces (8). In addition to pressure losses in the ribbed section of the channel, the pressure drop over the entire channel must include entrance and exit losses which are affected by the size and shape of the ports and gaskets. In the channels studied here, entrance and exit of the fluid was at right angles to the channel flow and in diagonally opposite corners.

In the work presented here experimental studies were conducted to determine the pressure drop across the ribbed section of rectangular channels with entrance and exit conditions similar to those in plate heat exchanger channels. The effects of rib and channel geometry were studied by varying the plate separation, rib frequency, rib base angle, rib shape, and transverse rib angle in twenty-four plastic plate channels.

EXPERIMENTAL APPARATUS AND PROCEDURE

The plastic plates used in this investigation were constructed of ⅜ in. plexiglas sheets, 32 in. long by 9½ in. wide. The various rib patterns were cemented to mating plates so that a channel could be formed by inserting a Neoprene rubber gasket between the plates. Three pressure taps were located at each end of the ribbed section to enable an average pressure drop across the ribbed section to be determined. A typical set of mating plates is shown in Figure 1.

Because of the many possible variations of rib geometry, several series of experiments, each designed to determine the effect of a single rib geometry on the pressure drop, were conducted. The effects of variations of plate separation and rib frequency were investigated using 45 deg. close-packed transverse triangular ribs. Plexiglas plates containing 30 and 60 deg. close-packed transverse triangular ribs were used to investigate the effect of the rib base angle. Transverse ribs with semicylindrical, trapezoidal, and square cross-sectional shapes were investigated because of their common usage in commercial equipment. The frequency of these ribs was chosen so that as uniform a channel spacing as possible was obtained. To increase the heat transfer area and induce further turbulence, the side slopes of 45 deg. close-packed transverse triangular ribs were corrugated in a direction transverse to the flow with step-by-step corrugations of 0.10 and 0.05 in. Another common commercial rib shape containing protrusions and depressions was investigated using semispherical shaped protrusions and depressions. Protrusions are semispherical bumps above the plate surface while depressions are semispherical holes below the plate surface.

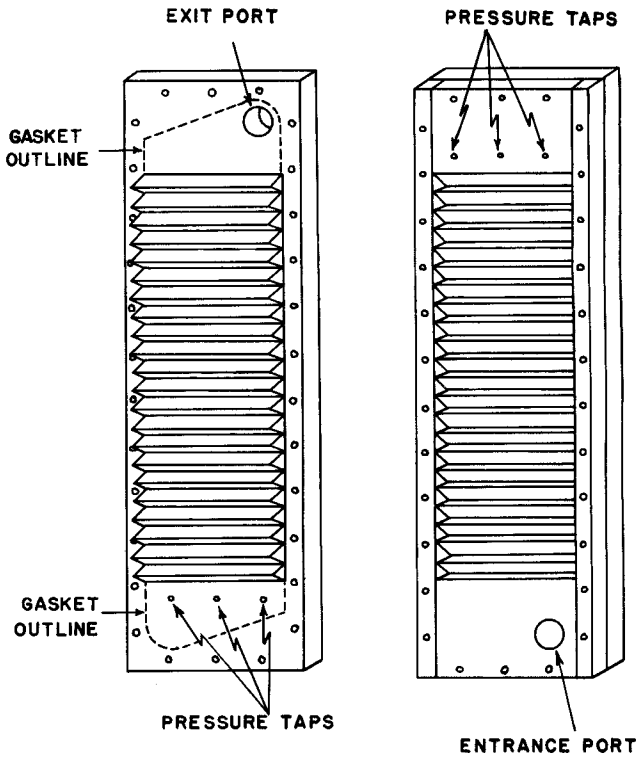

Fig. 1. Plexiglas channel plates.

In addition to the types of channels with transverse ribs, the ribs may be placed at some diagonal to the main flow stream. Most commercial plate heat exchangers with diagonal ribs have the ribs arranged in a herringbone pattern. The effects of this type of channel were investigated using 45 deg. close-packed triangular ribs arranged in a herringbone pattern with the ribs at 15, 30, and 45 deg. angles to the transverse. These plates were assembled in an interlocking manner as before and also in a noninterlocking manner with the diagonal or herringbone patterns on each plate crossed.

From the several investigations presented above, the effects of all aspects of rib and channel geometries on the pressure drop characteristics of plate heat exchanger channels were determined.

Basic dimensions of the rib geometries which were fabricated into channels and varied for plate separation and transverse rib angle are presented in Table 1.

For testing purposes, each plastic plate channel was assembled with a gasket and compressed in a specially constructed steel grid frame to provide a leakproof flow channel and to provide sufficient support to prevent plate buckling under pressure. The test section was connected to a fluid pumping and metering apparatus by specially constructed piezometer fittings at the entrance and exit ports. Water at 70 ± 2°F., used as the test fluid, was metered by several calibrated rotameters ranging from 0.1 to 40 gal./min. Pressure drops across the test section were measured by means of a manifold system connected to U-tube manometers with either mercury or carbon tetrachloride fluid according to the magnitude of the pressure drop.

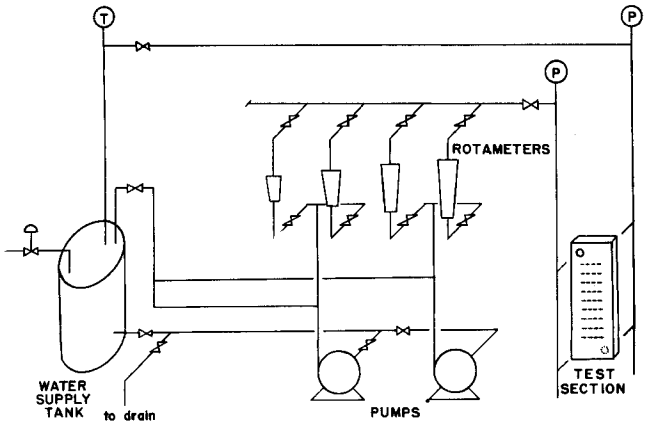

Fig. 2. Plexiglas channel study flow diagram.

TABLE 1. BASIC DIMENSIONS OF RIB GEOMETRY

Rib Dimensions	Height in.	Base in.	Frequency in.	Area sq. in.
45 deg. triangular	0.375	0.750	0.750	0.141
45 deg. triangular	0.375	0.750	1.500	0.141
45 deg. triangular	0.375	0.750	2.250	0.141
30 deg. triangular	0.216	0.750	0.750	0.081
60 deg. triangular	0.650	0.750	0.750	0.244
60 deg. trapezoidal	0.359	0.813	1.437	0.225
semicylindrical	0.375	0.750	1.375	0.221
square	0.250	0.250	1.250	0.125
corrugated	0.370	0.750	0.750	0.141
protrusions	0.250	0.500	1.250	0.098
protrusions	0.375	0.750	1.250	0.221

The plate separation or compressed gasket spacing was determined by measurement of the overall distance between the outer surfaces of the steel frame, with and without a gasket, at ten marked points. The difference of the average of the ten measurements, taken with a vernier depth gauge to 0.001 in., was used as the average plate separation.

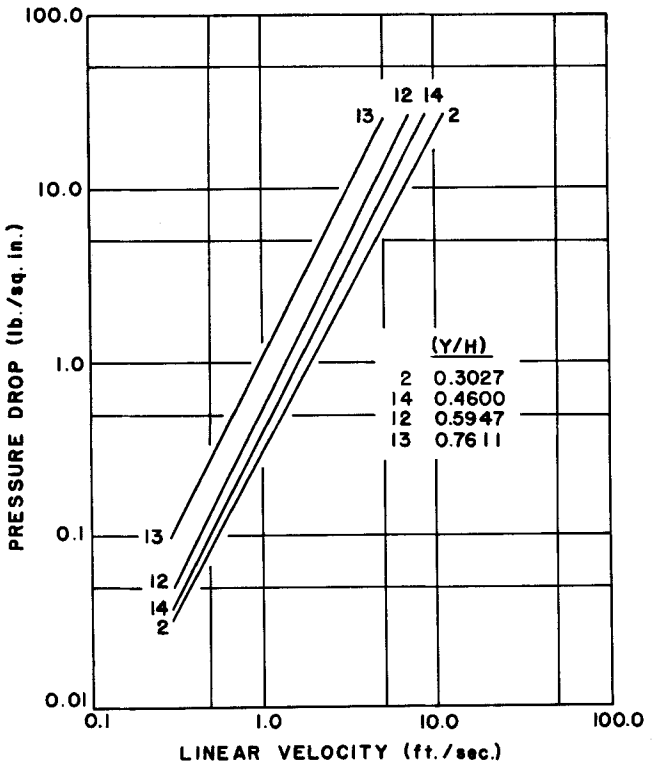

Fig. 3. Effect of plate separation on pressure drop, 45 deg. triangular interlocking ribs (Water, 70 ± 2°F.).

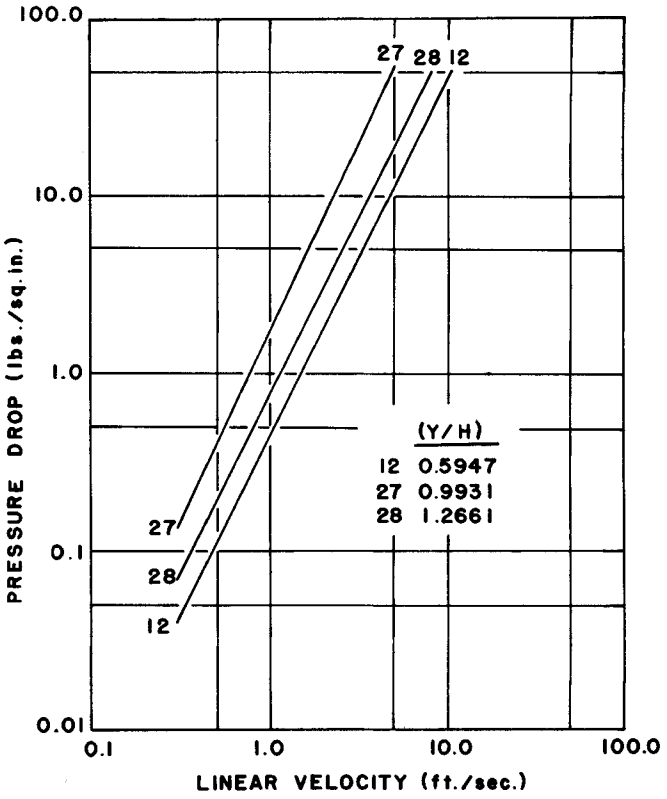

Fig. 4. Effect of plate separation on pressure drop, 45 deg. triangular noninterlocking ribs (Water, 70 ± 2°F.).

A diagram of the experimental apparatus is presented in Figure 2.

EFFECTS OF GEOMETRY ON PRESSURE DROP

The data taken for each plastic plate channel was correlated in the form, $\Delta p = a \cdot u^n$, by a least-squares fit of the experimental pressure drop data for the ribbed section of each channel investigated. Graphical representation of these results is presented in Figures 3 through 11. Since

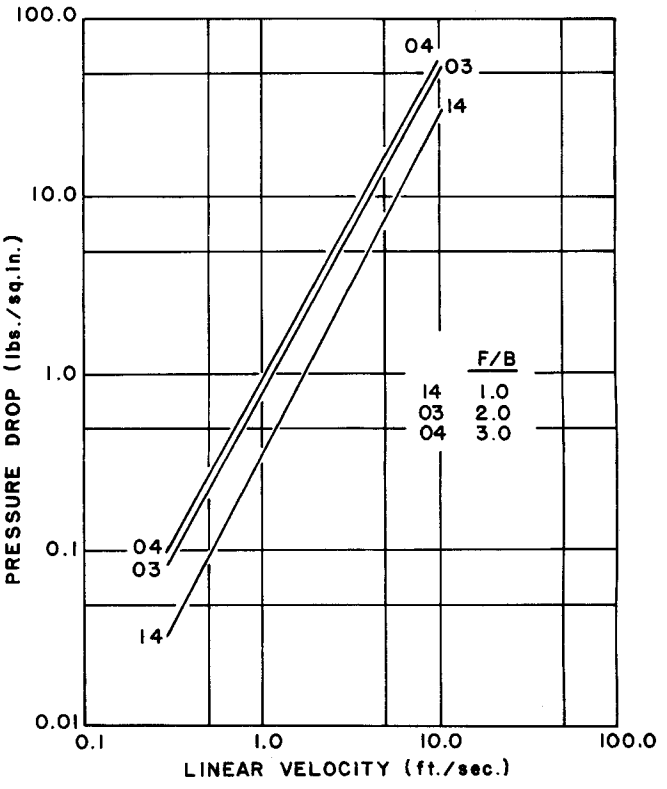

Fig. 5. Effect of rib frequency on pressure drop, 45 deg. triangular ribs (Water, 70 ± 2°F.).

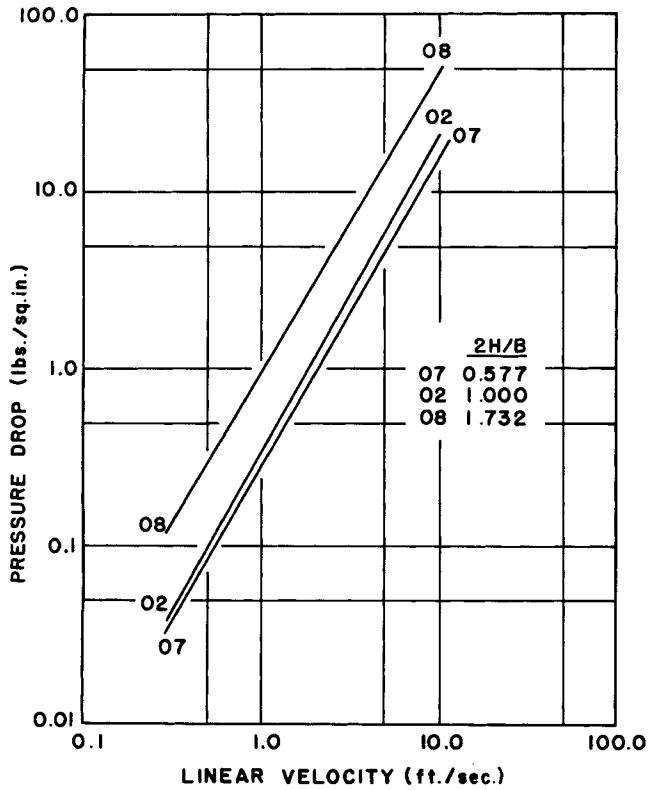

Fig. 6. Effect of rib base angle on pressure drop, close-packed triangular ribs (Water, 70 ± 2°F.).

only turbulent flow conditions were desired, only those data for linear fluid velocities above a range of minimum velocities of 0.15 to 0.30 ft./sec. were included for analysis. These minimum velocities correspond to critical Reynolds numbers (7) between 200 and 2,000 depending upon the plate channel in question. Because of the extremely small flow rates (less than 0.1 gal./min.) required to investigate laminar flow conditions with water, no attempt was made to interpret any data taken in the laminar region.

It has already been stated (5, 8) that pressure losses in ribbed channels are caused mainly by the eddy formations behind the ribs and changes in direction of the main flow around the ribs. Visual observations of the flow in the rectangular channels with the transverse internal geometries used in this work tend to support the observations that the turbulence is produced by a combination of the effects found in baffled and curved channels. The results shown in Figures 3 to 8 also support this type of flow phenomena.

From Figures 3 and 4 it can be seen that, at any constant linear velocity, the pressure drop increases as plate separation increases if the ribs on mating plates interlock ($Y/H < 1.0$). This may be attributed to an increase in eddy formation behind the ribs reinforcing the pressure loss present from curved channel flow. At plate separations where the ribs are noninterlocking ($Y/H > 1.0$), the pressure drop decreases at Y/H increases. A relative straightening of the main flow stream occurs here and the ribs behave more like roughness elements in baffled channels as the plate separation increases.

Figure 5 shows the pressure drop decreasing, at any constant linear velocity, as the ratio of rib frequency to rib base, F/B, increases from closepacked rib, $F/B = 1.0$ to $F/B = 3.0$. This change in channel geometry tends to straighten the main flow stream and also produce fewer eddies behind the ribs. An increase in pressure drop occurs when the base angle of the ribs increases from 30 to 60 deg. with a constant rib base dimension, B as shown in Figure 6. An increase in rib base angle also causes an increase in rib height, H, which tends to enhance eddy formation behind the ribs. As the shape of the ribs is changed from semicylindrical to trapezoidal to triangular and to square shapes, the pressure drop at any linear fluid velocity increases respectively as shown in Figure 7. Increasing the surface area of the ribs by corrugation also increases the pressure drop as shown in Figure 8. These step-by-step corrugations provide a rougher surface which further enhances eddy formation along the rib surface. Figure 9 indicates the effect of noncontinuous ribs and shows an increase in pressure drop as the degree of rib continuity increases. Figures 10 and 11 show the pressure drop increasing as the transverse angle of the herringbone ribs decreases from 45 to 15 deg. for both types investigated.

CORRELATION OF PRESSURE DROP

The results of the individual series of experiments on plastic plate channels were combined to establish a general expression for the pressure drop in the form:

$$\Delta p = K \cdot u^{\epsilon} \tag{5}$$

where

$$K = \Delta \cdot \Lambda \cdot B \cdot \Sigma \cdot \Gamma \cdot \Phi \cdot T \tag{6}$$

and

$$\epsilon = \delta \cdot \lambda \cdot \beta \cdot \sigma \cdot \gamma \cdot \phi \cdot \tau \tag{7}$$

In combining the individual correlations to form the general expression above, the correlations obtained for the 45 deg. triangular close-packed transverse rib patterns, Δ and δ, were taken as a basis. All other individual correlations were evaluated as fractions of that basis in such a way that, if any particular empirical correlation of channel geometry does not apply to the rib shape in question, that individual factor or fraction will be unity. The experimental results were also evaluated such that all effects of channel geometry were included in determining the individual effects of each geometric change.

Plate Separation

In the basic series of experiments conducted with the 45 deg. triangular close-packed transverse rib patterns, the

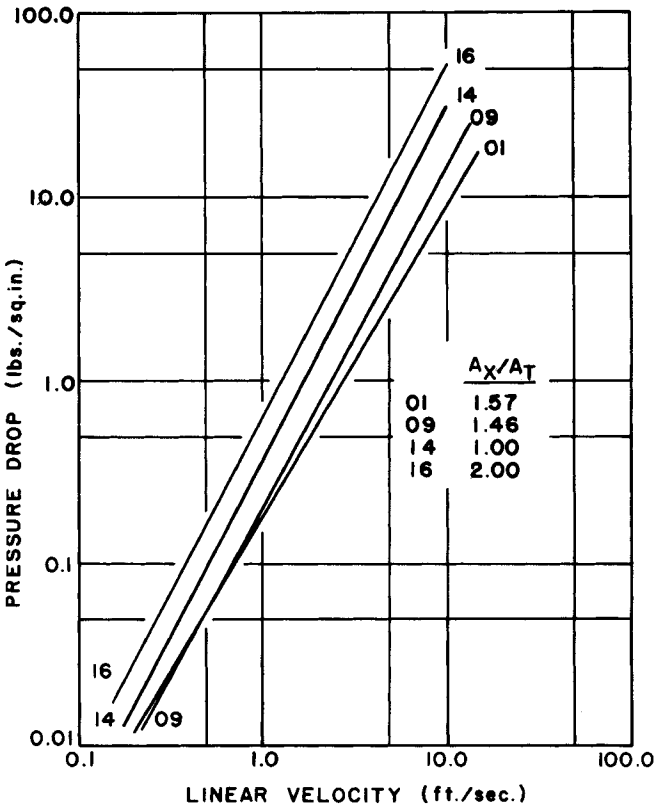

Fig. 7. Effect of rib shape on pressure drop (Water, 70 ± 2°F.).

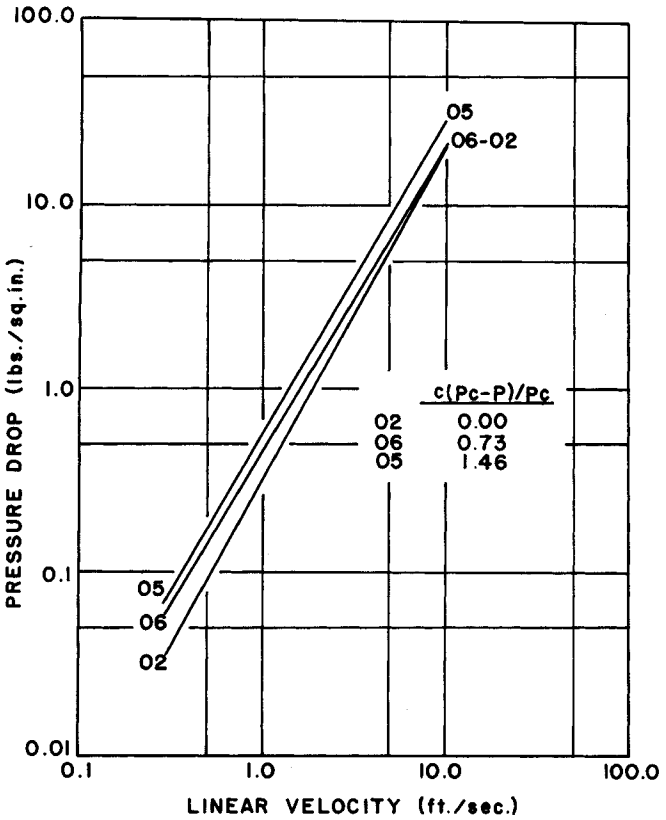

Fig. 8. Effect of rib corrugation on pressure drop, 45 deg. triangular ribs (Water, 70 ± 2°F.).

only independent characteristic of channel geometry varied was the plate separation, Y. The average channel spacing available for fluid flow, S, and the equivalent diameter of the channel, De, also varied but both are dependent on the plate separation, Y. Dimensionless parameters, Y/H and S/H, were selected for correlation in this series of experiments. Since H is the height of a rib, the parameter Y/H is a measure of the amount of interlock or overlap of the rib pattern. The parameter S/H is a measure of the space available for turbulent eddies to develop between successive ribs on opposite plates. Using only data for values of $Y/H < 1.0$, it was found that the effect of plate separation on the pressure drop could be evaluated by using the correlations

$$\Delta = -8.3081 + 8.6106 \cosh (S/H)^2 \qquad (8)$$

and

$$\delta = 1.0 + 1.3006 (Y/H)^{0.3935} \qquad (9)$$

for the coefficient, K, and the exponent, ϵ, in Equation (5). Use of these correlations to predict the pressure drop in the channels investigated provides an average deviation of +0.25% (±5.0% maximum) when comparing the experimental and predicted pressure drops for 150 individual data points.

Rib Frequency

To correlate the pressure drop as a function of the variation of the frequency of the ribs, the dimensionless parameter F/B was chosen in which F is the rib frequency or the distance between corresponding points of adjacent ribs and B is the base dimension of one rib. In this series of experiments, channels were constructed with 45 deg. triangular transverse ribs having F/B values of 1.0, 2.0, and 3.0. The following correlations were determined to express the effect of rib frequency on the pressure drop:

$$\Lambda = 1.0428 - 0.0428 \left(\frac{F}{B}\right)^{2.5} \qquad (10)$$

and

$$\lambda = 1.0 + 0.04 \sin^5 \left(\frac{\pi B}{F}\right) \qquad (11)$$

Using these correlations and the previously established correlations for the plate separation [Equations (8) and (9)] to predict the pressure drop in the channels investigated provides an average deviation of +2.2% (±4.4% maximum) when comparing the experimental and predicted pressure drops for 86 individual data *points*.

Rib Base Angle

The effect of rib base angle on the pressure drop was determined using close-packed transverse triangular ribs with base angles of 30, 45, and 60 deg. The dimensionless parameter, $2H/B$, is equal ot the tangent of the rib base angle for triangular shaped ribs. For other rib shapes, a numerical value for this parameter may be obtained even though it is not the tangent of the rib base angle. The correlations developed for use in Equation (5) are:

$$B = 0.2609 + 0.7391 (2H/B)^{2.5} \qquad (12)$$

and

$$\beta = 1.0718 - 0.0718 (2H/B)^{-2.0} \qquad (13)$$

An average deviation of +1.5% (±4.4% maximum) was obtained when using these correlations to predict the pressure drop in the channels investigated. Experimental and predicted pressure drops were compared for 94 individual data points.

Rib Shape

A series of experiments was conducted with triangular, semicylindrical, trapezoidal, and square transverse ribs to determine the effect of various rib shapes on the pressure drop. The variations of the channel geometry for this series of channels include those previously investigated (plate separation, rib frequency, and rib base angle) as well as the rib shape. To correlate the pressure drop as a function of the rib shape, the dimensionless parameter, A_X/A_T, was selected in which A_X is the cross-sectional area of the rib shape in question and A_T is the cross-sectional area of a triangle whose base and height dimen-

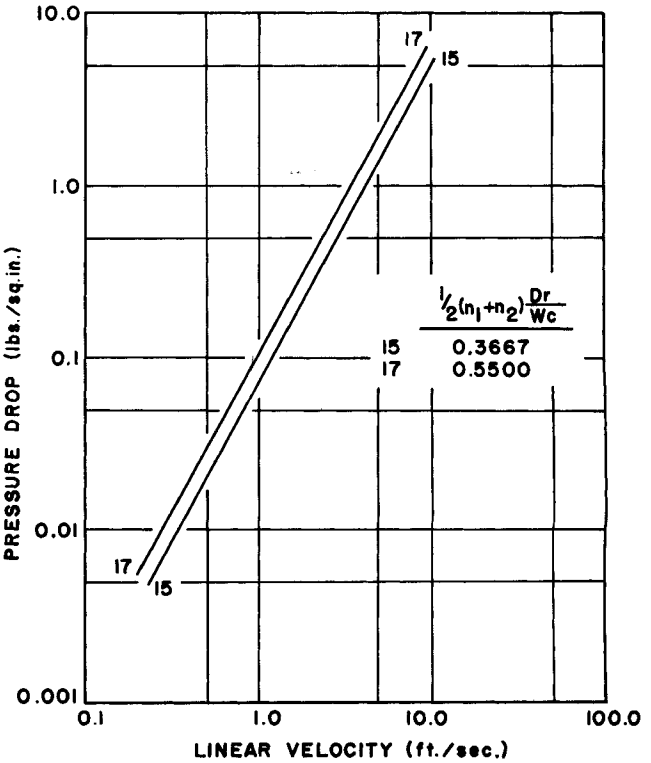

Fig. 9. Effect of semispherical protrusions on pressure drop (Water, 70 ± 2°F.).

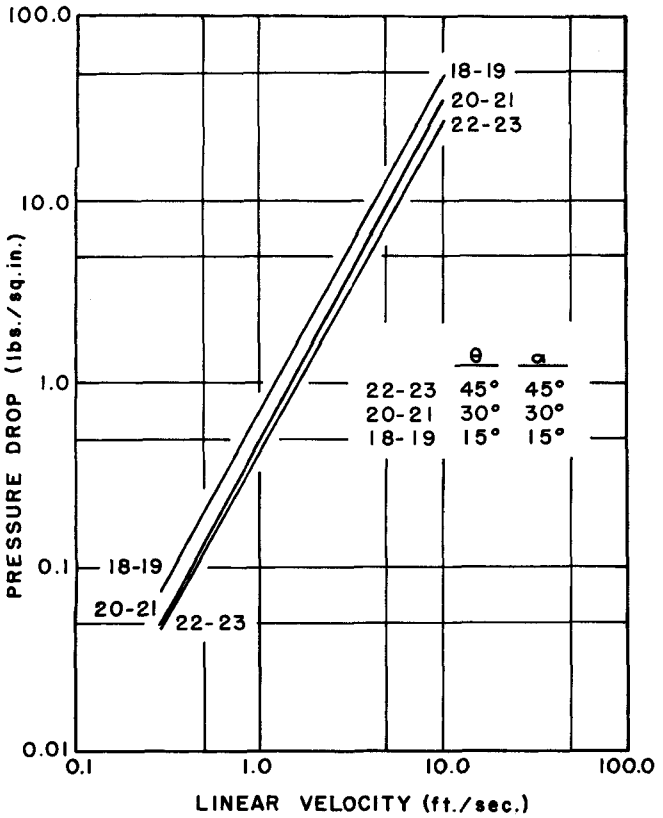

Fig. 10. Effect of transverse rib angle on pressure drop, interlocking herringbone ribs (Water, 70 ± 2°F.).

sion are the same as those of the rib shape in question. This ratio thus provides a parameter whose value will be unity for all triangular shaped ribs and greater than one for all other rib shapes. It was found that the effect of rib shape on the pressure drop could be evaluated by using the correlations

$$\Sigma = 1.04 - 0.562\cdot\psi + 0.15 \sin(2\pi\psi) - 0.08|\psi - 0.5| \quad (14)$$

and

$$\sigma = 1.0 - 0.07\psi + 0.15 \sin(2\pi\psi) \quad (15)$$

where

$$\psi = \frac{A_X}{A_T} - 1.0 \quad (16)$$

for the contribution of rib shape on the coefficient, K, and the exponent, ϵ, in Equation (5). Use of these correlations and those previously established to predict the pressure drop in the channels investigated provides an average deviation of +1.2% (±4.6% maximum) when comparing the experimental and predicted pressure drops for 114 individual data points.

Corrugated Ribs

The effect of rib corrugations on the pressure drop was determined by fabricating 45 deg. triangular ribbed channels with two different sized corrugations. To correlate the pressure drop as a function of the rib corrugations, the dimensionless parameter, $C(Pc - P)/Pc$, was selected in which C is one-half the number of corrugations on a rib surface, Pc is the lineal perimeter of the corrugated rib and P is the lineal perimeter of a noncorrugated rib with the same basic dimensions as the corrugated rib. Both perimeters, Pc and P, are measured on the rib surface along the direction of flow. This parameter is essentially a measure of the number of edges capable of inducing turbulence and the relative increase in surface area due to the corrugations. The correlations developed for use with Equation (5) are

$$\Gamma = 1.0 + 0.574\left(\frac{C(Pc - P)}{Pc}\right)^{0.6} \quad (17)$$

and

$$\gamma = 0.46 + 0.54\left(\left|\frac{C(Pc - P)}{Pc} - 1.0\right|\right)^{0.1} \quad (18)$$

An average deviation of +0.8% (±4.4% maximum) was obtained when using these correlations to predict the pressure drop in the channels investigated. Experimental and predicted pressure drops were compared for 86 individual data points.

Protrusions

A series of experiments was conducted with ½ and ¾ in. semispherical protrusions and depressions to determine the effect of noncontinuous ribs on the pressure drop. To correlate the pressure drop as a function of the size of the protrusions, the dimensionless parameter, $\frac{1}{2}(n_1 + n_2)\,Dr/Wc$, was selected in which n_1 and n_2 are the number of protrusions in two successive transverse rows, Dr is the diameter or transverse dimension at the base of a protrusion and Wc is the transverse width of the channel between gaskets. This parameter is, in effect, a measure of the rib continuity or the amount of transverse flow area taken up by a rib. The correlations developed for use with Equation (5) are:

$$\Phi = e^{-3.9\{1.0 - [1/2(n_1+n_2)Dr/Wc]^{0.3}\}} \quad (19)$$

and

$$\phi = 0.59 + 0.41\left[\frac{1}{2}(n_1 + n_2)\frac{Dr}{Wc}\right] \quad (20)$$

Use of these correlations and the previously established correlations to predict the pressure drop in the channels investigated provides an average deviation of +0.9% (±11.6% maximum) when comparing the experimental and predicted pressure drops for 82 individual data points.

Transverse Rib Angle

The effects produced by positioning the ribs at various

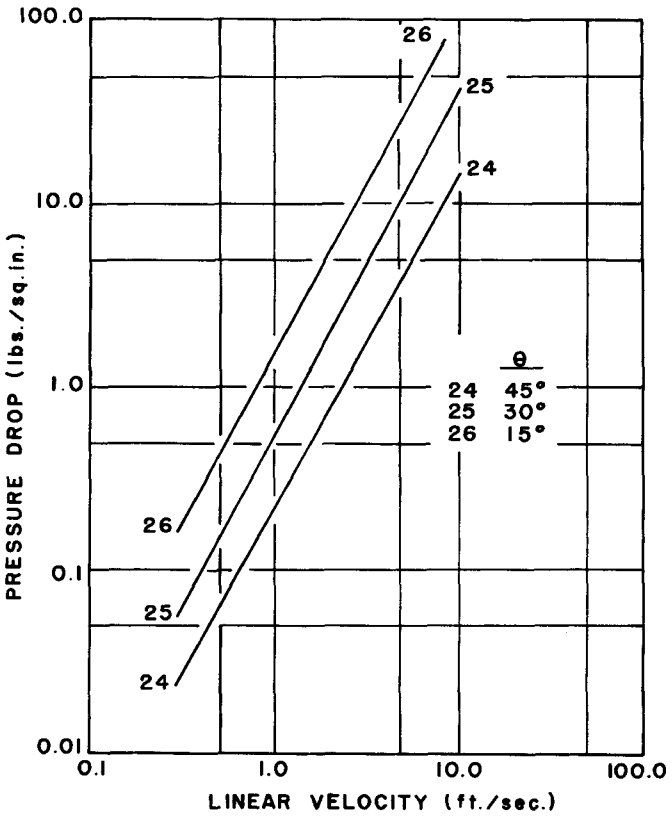

Fig. 11. Effect of transverse rib angle on pressure drop, noninterlocking herringbone ribs (Water, 70 ± 2°F.).

angles to the transverse flow direction was determined by conducting a series of experiments with 45 deg. triangular close-packed ribs arranged in a herringbone pattern. For this series of experiments, herringbone rib patterns with transverse angles of 15, 30, and 45 deg. were investigated with both interlocking and noninterlocking or crossed rib channels. Because of the more complex situation existing with nontransverse ribs, the parameter chosen for correlation was the transverse rib angle, θ. The interlocking herringbone rib patterns were investigated with the fluid flowing both into and against the apex of the herringbone pattern. It was found that these different directions of flow produced a maximum difference of only 2% and were therefore neglected in the final correlations. So that the effects of both interlocking and noninterlocking rib patterns could be combined into a single correlation; an angle, α, equal to the transverse rib angle, θ, was defined for the interlocking rib patterns. For the noninterlocking rib patterns, the angle α is equal to zero. The correlations developed for use with Equation (5) are:

$$T = [1.0 + 8.5 \tan^{1.75}\alpha][1.0 - 1.33 \sin\theta + 0.103 \sin(2.54\,\pi\theta)] \quad (21)$$

$$\tau = 1.0 - 0.18\left(\frac{\theta}{\alpha + \theta}\right)^{1.75} \quad (22)$$

Using these correlations and the previously established correlations to predict the pressure drop in the channels investigated provides an average deviation of +1.0% (±11.9% maximum) when comparing the experimental and predicted pressure drops for 228 individual data points.

APPLICATION OF RESULTS

The results of this investigation were used to test the possibility of predicting the pressure drop in commercial plate heat exchanger channels. Overall pressure drop data, including entrance and exit effects, were available from an investigation of commercial plate heat exchanger channels (8). Using the geometric characteristics of the commercial heat exchanger plates with the empirical correlations developed from the plexiglas channels used in this investigation, ribbed section pressure drops for the commercial metal plate channels were predicted. A typical example of the comparison between the overall pressure drop in a commercial plate channel and the predicted ribbed section pressure drop for the same channel is presented in Figure 12.

To provide some means of quantitatively comparing these results average entrance and exit pressure losses were added to the predicted ribbed section pressure drops. In this investigation with plexiglas channels, entrance and exit effects were found to be about 20% of the ribbed section pressure drop (10% of the total pressure drop) for most of the channels investigated. This result is based on the 1½ in. diameter circular port and the one gasket shape (Figure 1) used in this work. Although the entrance and exit conditions of all commercial plates are quite different than those of the plexiglas models, the overall pressure drops for seven commercial plate channels were predicted with an average deviation of 41.5% from experimental overall pressure drops. The experimental pressure drop data showed an average deviation of 44.4% for the seven exchangers considered (18). These results show the predicted pressure drop data to be at least as good as the experimental data used for comparison.

Additional applications of this investigation with respect to heat transfer in ribbed channels will be presented in a subsequent paper.

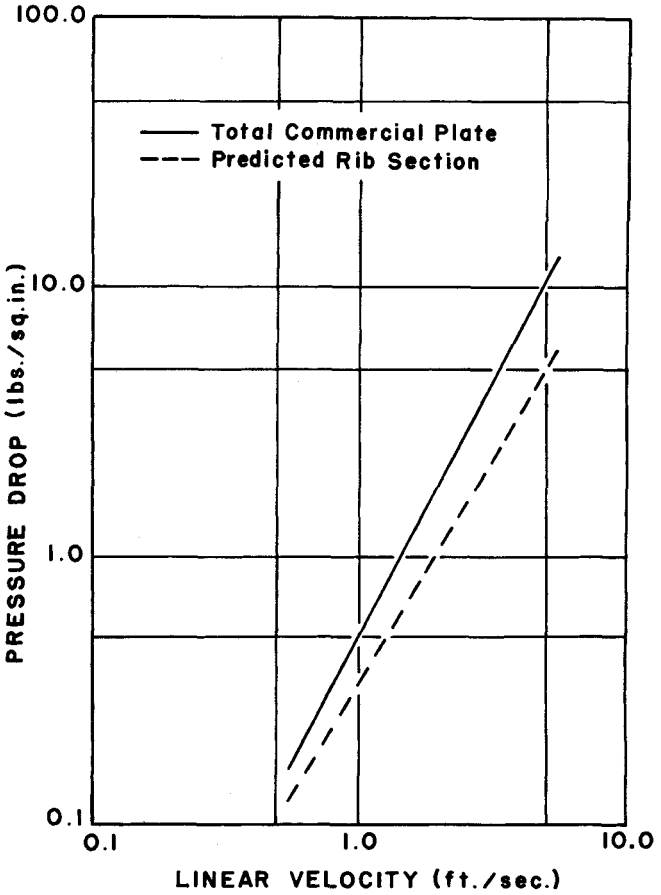

Fig. 12. Typical comparison of predicted rib section and overall commercial plate pressure drops.

CONCLUSIONS

Based on the results reported in this work within the range of the variables investigated, it may be concluded that:

1. The pressure drop in rectangular ribbed channels is governed by the geometry of the ribs and the channel.
2. The mathematical correlations developed may be used to predict the pressure drop in rectangular ribbed channels similar to those investigated in this work.
3. The pressure drop in plate heat exchanger channels operating with fluids similar to water may be predicted using the correlations presented here if one also includes an accurate estimate of the entrance and exit effects.

ACKNOWLEDGMENT

The authors gratefully acknowledge the cooperation of the Northeastern University Computation Center, the assistance of William J. Duffy in collecting some of the experimental data, the fellowship support received from the Esso Foundation and N.D.E.A. for Dr. Ralph A. Buonopane, and a grant-in-aid received from Hercules Inc. for the purchase of accessory experimental equipment.

NOTATION

a = coefficient in experimental correlation, $\Delta p = a \cdot u^n$
A = coefficient in experimental correlation, $N_{Eu} = A \cdot N_{Re}{}^{-N}$
A_X = cross-sectional area of any nontriangular rib, sq. in.
A_T = cross-sectional area of any triagular rib, sq. in.
B = dimension of rib base, in.
C = one-half the number of corrugations on a rib surface
De = equivalent diameter of channel, ft.
Dl = developed length of plate surface, ft.

Dr = transverse base dimension of a rib, in.
f_B = Blasius friction factor, $2 \cdot \Delta p \cdot g_c \cdot De/\rho \cdot u^2 \cdot Dl$, dimensionless
F = rib frequency or distance between corresponding points of successive ribs, in.
g_c = gravitational constant, 32.2 ft.lb.$_m$/lb.$_f$ sq. sec.
H = height of a rib or internal geometry, in.
K = coefficient in empirical correlation, $\Delta p = K \cdot u^{\epsilon}$
n = exponent in experimental correlation, $\Delta p = a \cdot u^n$
n_1 = number of ribs in a transverse row succeeding n_2
n_2 = number of ribs in a transverse row succeeding n_1
N = exponent in experimental correlation, $N_{Eu} = A \cdot N_{Re}{}^{-N}$
N_{Eu} = Euler number, $\Delta p \cdot g_c/\rho \cdot u^2$, dimensionless
N_{Re} = Reynolds number, $De \cdot u \cdot \rho/\mu$, dimensionless
Δp = pressure drop, lb./sq.in.
P = lineal perimeter of a noncorrugated rib, in.
Pc = lineal perimeter of a corrugated rib, in.
S = average plate spacing for fluid flow, in.
u = lineal fluid velocity in channel, ft./sec.
Wc = transverse width of plate channel between gaskets, in.
Y = plate separation or compressed gasket thickness, in.

Greek Letters

α = transverse rib angle for cross diagonal ribs, $\alpha = \theta$, radians
β' = exponent correlation for rib base angle effects
β = base angle of ribs, radians
B = coefficient correlation for rib base angle effects
γ = exponent correlation for rib corrugation effects
Γ = coefficient correlation for rib corrugation effects
δ = exponent correlation for plate separation effects
Δ = coefficient correlation for plate separation effects
ϵ = exponent in empirical correlation, $\Delta p = K \cdot u^{\epsilon}$
θ = transverse rib angle for diagonal ribs, radians
λ = exponent correlation for rib frequency effects
Λ = coefficient correlation for rib frequency effects
ρ = density of fluid, lb./cu.ft.
σ = exponent correlation for rib shape effects
Σ = coefficient correlation for rib shape effects
τ = exponent correlation for transverse rib angle efects
T = coefficient correlation for transverse rib angle effects
ϕ = exponent correlation for protrusions
Φ = coefficient for protrustions
ψ = rib shape geometrical parameter, $A_X/A_T - 1.0$, dimensionless

LITERATURE CITED

1. Troupe, R. A., J. C. Morgan, and J. Prifti, *Chem. Eng. Progr.*, **56**, No. 1, 124 (1960).
2. Seligman, R. J. S. and G. A. Dummett, *Chem. Ind,*. No. 38, 1602 (1964).
3. Baranovskii, N. V., "Plate-Type Heat Exchangers," pp. 122 to 148, Moscow, U.S.S.R. (1962).
4. Watson, E. L., A. A. McKillop, and W. L. Dunkly, *Ind. Eng. Chem.*, **52**, No. 9, 733-40 (1960).
5. Smith, V. C., and R. A. Troupe, *AIChE J.*, **11**, 487 (1965).
6. Maslov, A., *Molochnaya Promyshlennost*, **24**, No. 6, 17 (1963).
7. ———, *Pishchevaya Tekhnologiya*, No. 5, 143 (1964).
8. Buonopane, R. A., Ph.D. thesis, Northeastern Univ., Boston, Mass. (1967).

Manuscript received January 12, 1968; revision received April 22, 1968; paper accepted April 24, 1968.

Part II. Heat Transfer

Heat transfer and pressure drop data were taken on commercial plate heat exchange equipment. Nusselt and Euler correlations were determined for each of the six commercial heat exchangers investigated. These correlations were combined to establish a single heat transfer-pressure drop relationship for any plate type of heat exchanger channel.

The results of this investigation were tested by using the correlations developed in Part I of this series to predict pressure drop data for the commercial unit based on their channel geometries. These predicted pressure drops were then used with the results of this part of the series to predict and compare heat transfer data.

The correlations developed in this work allow one to determine the heat transfer characteristics in a ribbed rectangular channel from the pressure drop characteristics of the channel in question.

The effects of internal geometries on the pressure drop in ribbed rectangular channels have been correlated as functions of the rib and channel geometry in Part I of this series. Although the heat transfer characteristics of such channels are governed by the flow conditions, no attempts to correlate the heat transfer with pressure drop characteristics appear in the literature. Combined correlations relating heat transfer and pressure drop conditions have been determined for other types of turbulence producing channels (*1, 2*). This paper presents results which, when combined with those reported in Part I, will enable one to predict heat transfer characteristics from pressure drop conditions based on the rib and channel geometry.

In an investigation of flow in annuli containing finned turbulence promoters on the outer surface of the inner tube, Knudsen and Katz (*1*) obtained an empirical correlation containing dimensionless ratios of the fin height and spacing to the equivalent diameter of the channel. Sams (*2*), in an investigation of air flowing in ½ in. circular tubes with square-thread roughness elements on the inner surface, developed a friction factor correlation containing dimensionless ratios of the thread spacing and height to the thread width. He incorporated this friction factor into the Reynolds number group of an empirical Nusselt correlation thus combining the heat transfer and pressure drop correlations.

Extensive heat transfer studies have been conducted on plate and frame equipment (*3, 5* to *9*) all of which present results in the form of Nusselt correlations applicable to each individual exchanger investigated. The most complete presentation of Nusselt and Euler correlations for plate heat exchangers appears in Baranovskii's work (*3*). In all of the works cited above, the empirical Nusselt correlations are used only for the thermal design characteristics of the heat exchanger in question. Both Baranovskii (*4*) and Kovalenko (*10*) derive the correlation

$$\frac{\zeta}{2} \cdot \frac{u^2}{2 \cdot g_c \cdot Hp} \cdot \frac{Y}{Dl} \cdot \frac{t_2 - t_1}{\Delta t_{lm}} \cdot \frac{Cp \cdot \rho \cdot u}{U_{\text{avg.}}} = 1 \qquad (1)$$